

AUTOMATED WIRELESS DRONE CHARGING STATION

By

Samuel Fakunle

Pranshu Teckchandani

Jason Wuerffel

Final Report for ECE 445, Senior Design, Spring 2024

TA: Matthew Qi

May 2024

Project No. 29

Abstract

For our senior design project, we decided to make an automated wireless drone charging station. The main purpose of this project is to successfully charge a drone when then drone lands on the charging pad without human intervention. The charger takes in 24V DC power supply from a battery and charges the battery on the drone. The system has many components like a resonant tank, an AC-DC converter, a buck converter, and others. We were able to successfully demonstrate the wireless power transfer and operate the system within the defined limits. However, we couldn't get the high side circuitry of the gate driver to work and so we weren't able to demonstrate the working of the entire system at high voltages. Despite this challenge, our project lays a solid foundation for the development of efficient and autonomous drone charging systems.

Contents

- 1. Introduction1
 - 1.1 Problem1
 - 1.2 Solution1
 - 1.3 Visual Aid1
 - 1.4 High Level Requirements2
- 2 Design.....3
 - 2.1 Physical Design.....3
 - 2.2 Block Diagram3
 - 2.2.1 Subsystem 1: Two step inverter and voltage regulation4
 - 2.2.2 Subsystem 2: Resonant Coils6
 - 2.2.3 Subsystem 3: Full Bridge Rectifier7
 - 2.2.4 Subsystem 4: Synchronous Buck Converter with Voltage Regulation8
 - 2.2.5 Subsystem 5: Micro Controller Unit8
- 3. Design Verification10
 - 3.1 Two Step Inverter and Voltage Regulation10
 - 3.2 Resonant Coils.....10
 - 3.3 Full Bridge Rectifier.....11
 - 3.4 Synchronous Buck Converter with Voltage Regulation12
 - 3.5 Microcontroller Unit13
- 4. Costs.....15
 - 4.1 Parts15
 - 4.2 Labor17
- 5. Conclusion.....18
 - 5.1 Accomplishments and Uncertainties18
 - 5.2 Ethical considerations18
 - 5.3 Future work.....19
- References20
- Appendix A Requirement and Verification Table22

1. Introduction

1.1 Problem

Drone technology is becoming more vital for our modern society because it improves productivity and precision for several applications. Despite this, the operation time continues to be a key technological challenge because of the drone's battery life limitations. As a result, our project aims to address this issue by implementing an automated drone charging system that extends the drone's flight time without human intervention.

1.2 Solution

Our group aims to use resonant inductive coupling to develop a wireless drone charging station that allows the drone to land and charge its battery within an acceptable distance from the transmitter. The combination of the coils on the drone and on the charging pad will essentially act as an air gap transformer. Circuitry leading up to the coil on the charging pad side will consist of a power source, full bridge synchronous rectifier, and resonant tank. Circuitry after the transformer on the drone side will include an AC-DC converter followed by a synchronous buck converter and ending with a BMS. Our system should start power transfer only when the drone lands in close proximity to the coil on the pad. An MCU will be used to provide PWM to the gate driver that drives MOSFETs used throughout the project based on inputs from a proximity sensor.

1.3 Visual Aid

The design for our system was based on the image shown in Figure 1. For our final design, we created a charging pad which had the transmitting coil and a stand which emulated a drone. We had a receiving coil attached to it and the battery was supposed to be placed on top of the stand. Our final product design can be seen in Figures 2. Figures 3 and 4 show a detailed image of the transmitting and receiving side of our design.



Figure 1: Initial inspiration for our design

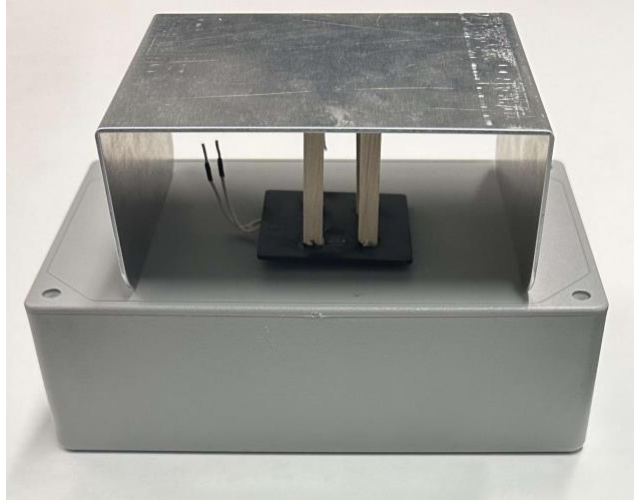


Figure 2: Final product

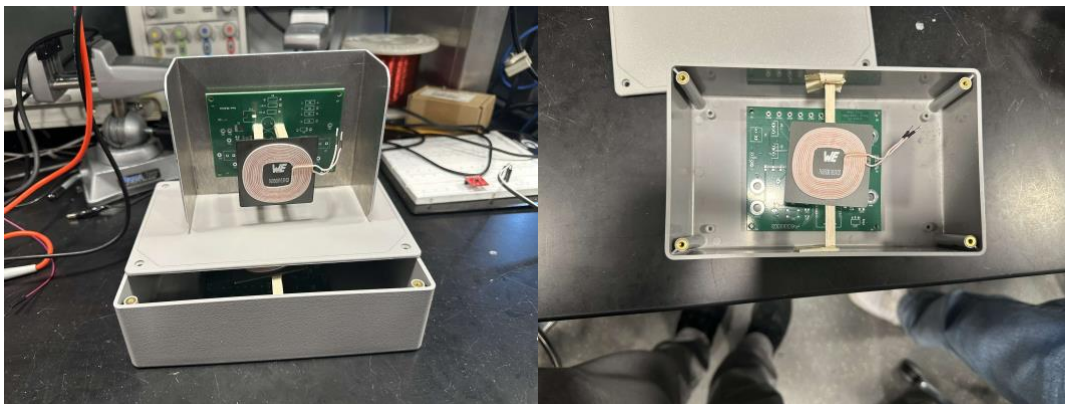


Figure 3 and 4: Figure 3 (left) shows the receiving side of the charger. It shows the bottom of the stand we created to emulate a drone. Figure 4(right) shows the inside of the charging pad which has the transmitting coil

1.4 High Level Requirements

Our system has four high level requirements. These requirements have been drafted after careful consideration and they encompass several key aspects of our system.

1. The system can supply $3.8V \pm 3\%$ V DC to 1S LiPO battery, when supplied with 24V DC power from the power supply.
2. The charging pad can charge the drone to at least 90% of the maximum battery capacity without human interference with an efficiency of at least 50% only after the coils are within the set proximity of 5 cm.
3. The system should be able to operate up to a resonant frequency of 125kHz.
4. The system should operate within the 0.97dB range (Power produced by the resonant tank is between P_{max} and $0.8 * P_{max}$).

2 Design

2.1 Physical Design

Before we discuss the block diagram and the design of the entire system, let us quickly go over the physical design of the charging pad. The figure below shows the dimensions of the box we used to keep the transmitting coil.

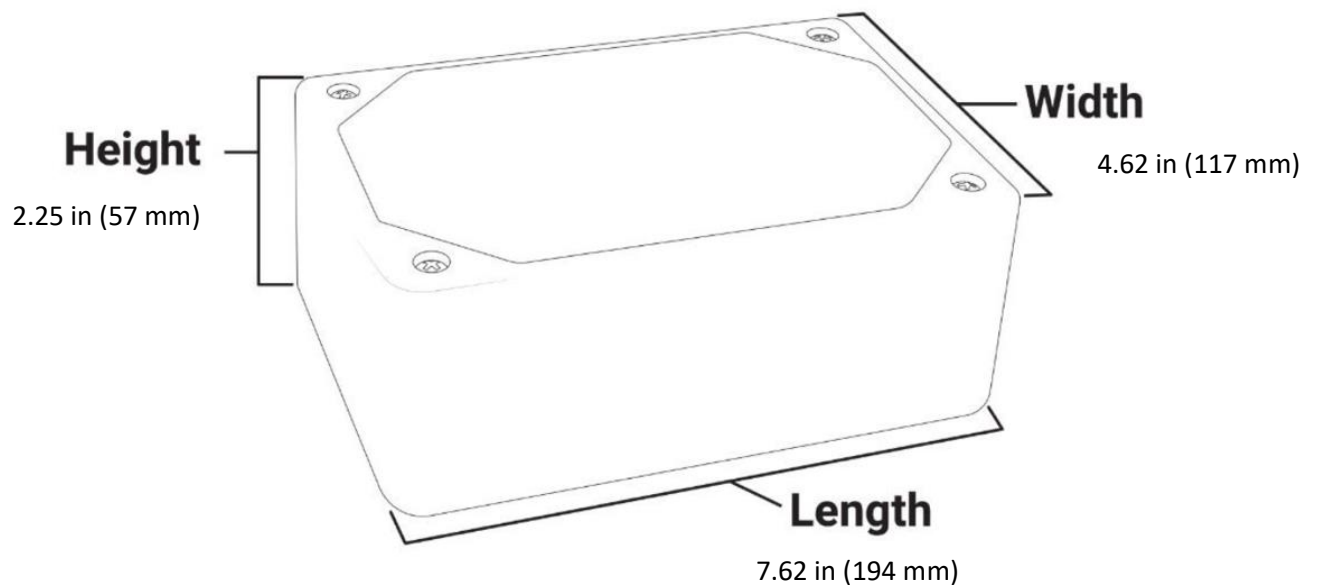


Figure 5: Dimensions of the box used for the charging pad

The stand that which acted as a drone was made by the machine shop and the dimensions for that were 150x 100 x 55mm.

2.2 Block Diagram

The final block diagram for our system is shown in Figure 6. This diagram shows all the subsystems of our system and how they are connected to each other. You can see that the input for our system is a 24V DC voltage source and the output is being used to charge a 1S LiPO battery with a voltage rating of 3.7V. Subsystems 1,2 and 5 are placed on the PCB on the transmitting side(charging pad) and the remaining systems are on the receiving side PCB (Drone Side). The design of each of the subsystems in explained in detail in the following subsections.

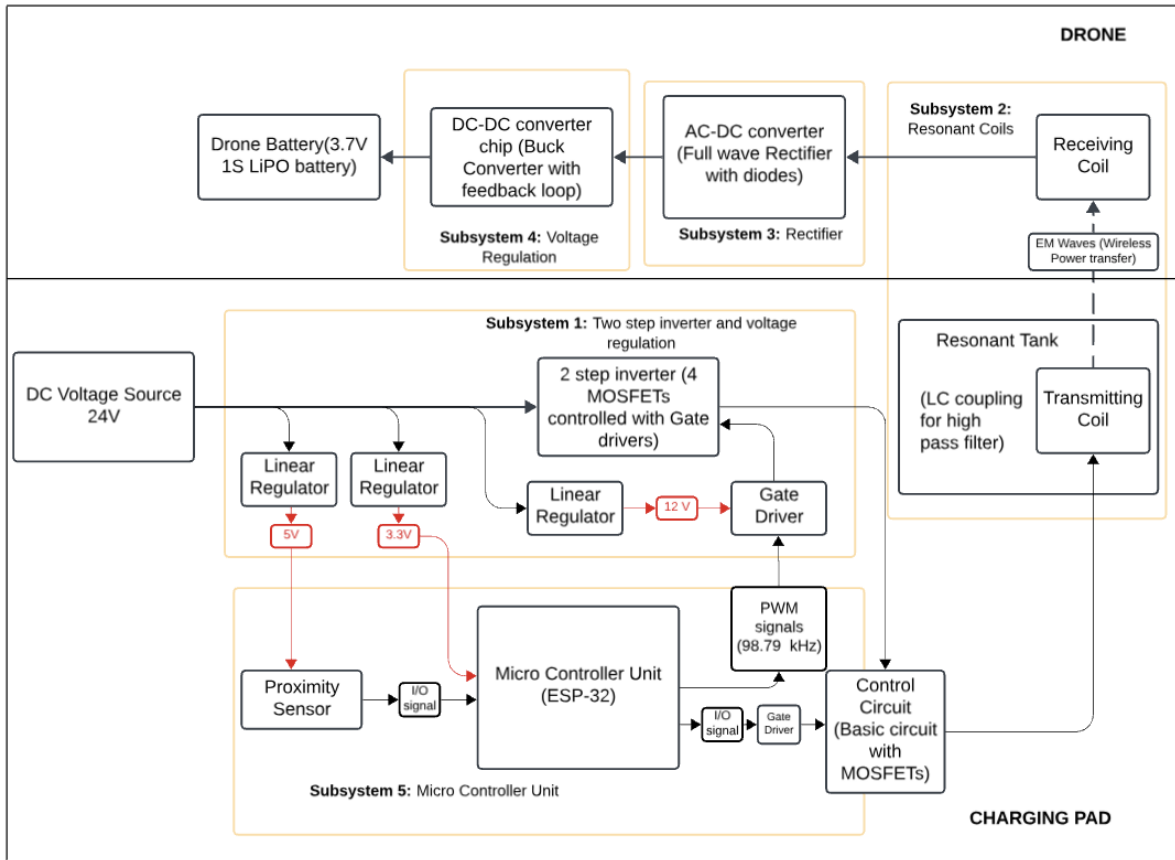


Figure 6: Block Diagram

2.2.1 Subsystem 1: Two step inverter and voltage regulation

This subsystem consists of a 24V DC power supply and a full bridge inverter circuit. We also provide power to the transmitter of the proximity sensor, the MCU and the gate driver as a part of this subsystem.

Voltage Regulation:

This subsystem consists of 3 different voltage regulators. The voltage regulators are used to output voltage of 3.3V (for the MCU), 5V (for the 2 proximity sensors), and 12V (for the gate driver). Figure 7 shows the circuit schematic for all three of the voltage regulators.

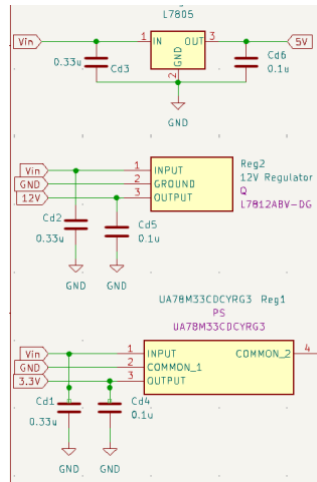


Figure 7: Voltage Regulators

Inverter Circuit:

Our inverter circuit consists of four MOSFETs as seen in the figure. The circuit takes input from a 24V DC Power Supply and it outputs a square wave. This is a 2 step inverter meaning the output will only have two voltage values -24V and 24V. The inverter circuit will be based on the following topology.

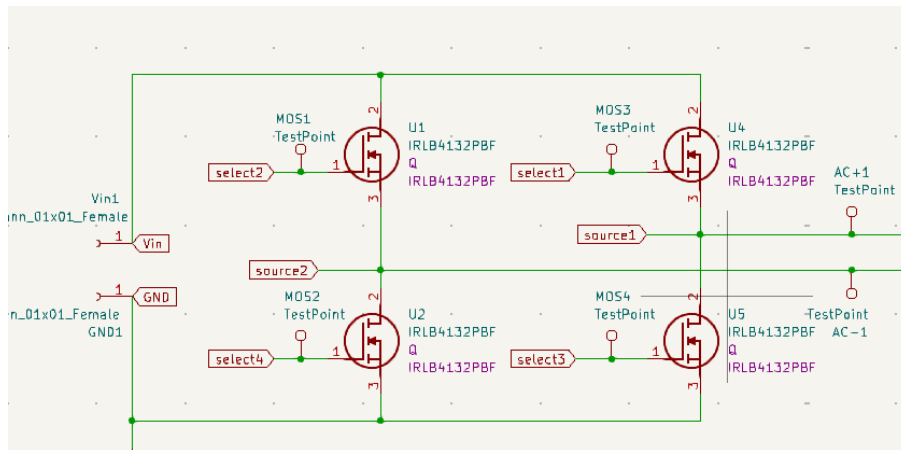


Figure 8: Bridge inverter

The MOSFETs will be controlled by complementary PWM signals (100 kHz frequency) which will be generated by gate driver ICs. Gate signals select2 and select2 are outputs from the high side circuitry of the gate driver and the remaining two gate signals are outputs from low side circuitry of the gate driver.

This subsystem also consists of three linear regulators, which take in 24V from the DC power source and output 3.3V, 3.3V and 12V. The two 3.3V outputs are used to power devices in subsystem 5 (proximity sensors and MCU) while the 12 V is used to power the gate driver used to amplify the PWM signals to the MOSFETs. The circuit for the gate driver is as follows:

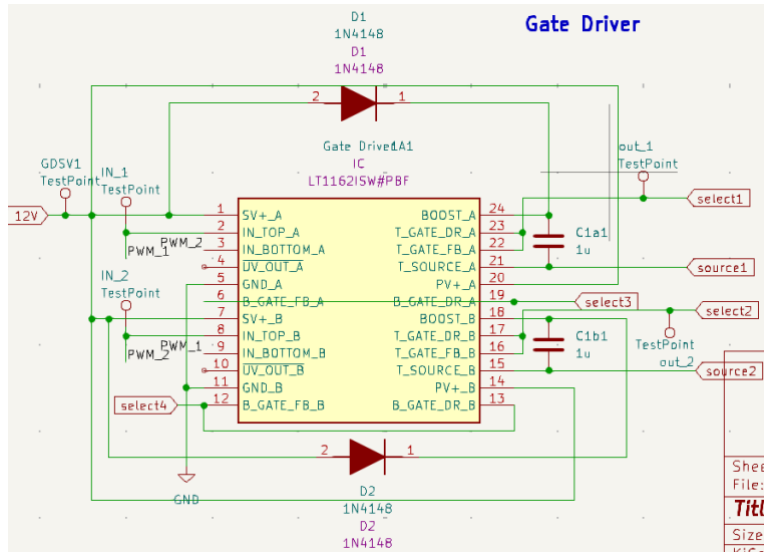


Figure 9: Gate driver circuit

The input for the gate driver is coming from the ESP-32. A gate driver is used to amplify the voltage levels of the PWM signals so that they can effectively trigger the MOSFETs. This implementation of the gate driver is inspired by the application circuit provided in the datasheet for the Gate Driver [16].

2.2.2 Subsystem 2: Resonant Coils

This system consists of the LC Resonant tank and the transmitting and the receiving coils. The LC coupling will be used as a band pass filter for the incoming square wave. The Inductance over here will be the inductance of the transmitting coil. The circuit is designed to output a AC waveform on the receiving side. The schematic for this subsystem will be like the following figure:

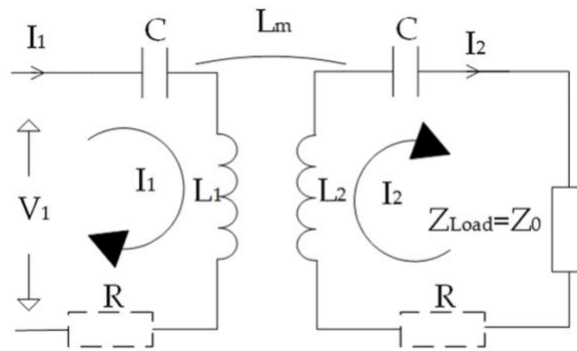


Figure 10: Coil network with LC resonant tank

The left side is the transmitting side. The input to the transmitting side is a square wave. L_1 represents the inductance of the transmitting coil. The capacitor is chosen in such a way that the resonant frequency of the circuit is equal to within 0.97dB of the frequency of maximum power transmission. For our design, we won't be including the capacitor on the receiving side (right side). The resistances indicate the resistances of the wires and L_2 indicates the inductance of the receiving coil. L_m is the mutual inductance.

The main thing in this subsystem is to keep the quality factor of the LC circuit high to ensure that the waveform for wireless power transmission is of high frequency. For our set of transmitting coils, the bode plot looked as follows. The peak is at 125kHz which was verified by us by testing in the lab. Our system is working at 100kHz which is within the 0.97dB range.

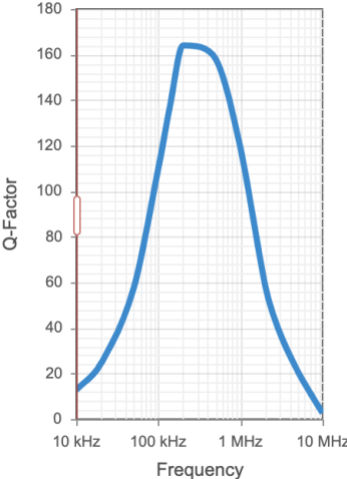


Figure 11: Bode plot

We are aiming for a frequency within the 0.97dB range. This would mean that the power outputted by the Resonant tank would be within P_{max} and $0.8 * P_{max}$ (P_{max} being the maximum power output at 125kHz).

Another factor to consider here is the coupling coefficient of the coils. The coupling coefficient depends on the individual inductances of the coils and the mutual inductance.

2.2.3 Subsystem 3: Full Bridge Rectifier

This subsystem includes a full bridge rectifier with a filter, which is responsible for converting AC voltage from receiving coil to 10V DC. Our target AC voltage from the receiving coil is $12 \pm 3\%$ V AC, but this may vary depending on the electrical characteristics of the coils, especially the coupling factor. Our capacitive filter would be flexible enough to account for unexpected variations. The filter would include a capacitor tank to allow for more flexibility. The rectifier would utilize four 1N4007-T diodes, hence communication with ESP32 microcontroller is not required.

The figure below shows our schematic for the full bridge rectifier:

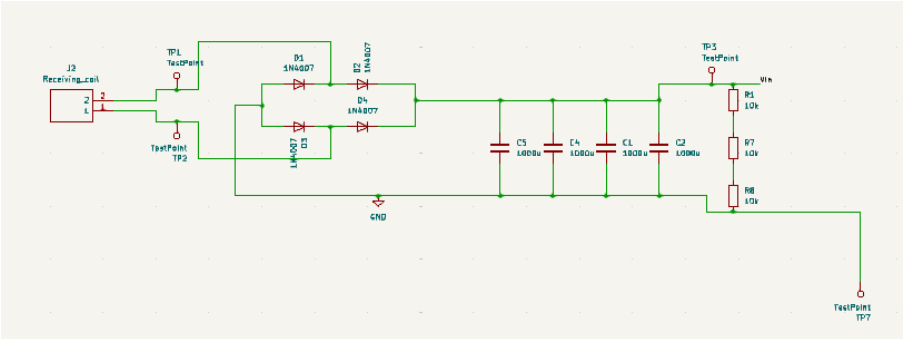


Figure 12: Full Bridge Rectifier

2.2.4 Subsystem 4: Synchronous Buck Converter with Voltage Regulation

This subsystem includes a TPS54335ADDAR (TI) synchronous buck converter chip responsible for converting $10 \pm 3\%$ V DC to $3.8 \pm 3\%$ V DC for the drone's battery. We will rely on the current mode control capabilities of the chip to perform output voltage dynamic regulation. The chip achieves this by comparing the output voltage to a reference voltage through an error amplifier [9]. The output of the error amplifier is then used to switch the high side MOSFET [9]. The chip also utilizes slope compensation to ensure that the peak inductor current is constant, particularly when the duty ratio of the switches is increased during dynamic regulation [9]. Both control schemes are vital to ensure effective and safe charging of the drone's battery in all scenarios, thus ensuring system stability.

The figure below shows a schematic for the synchronous buck converter chip:

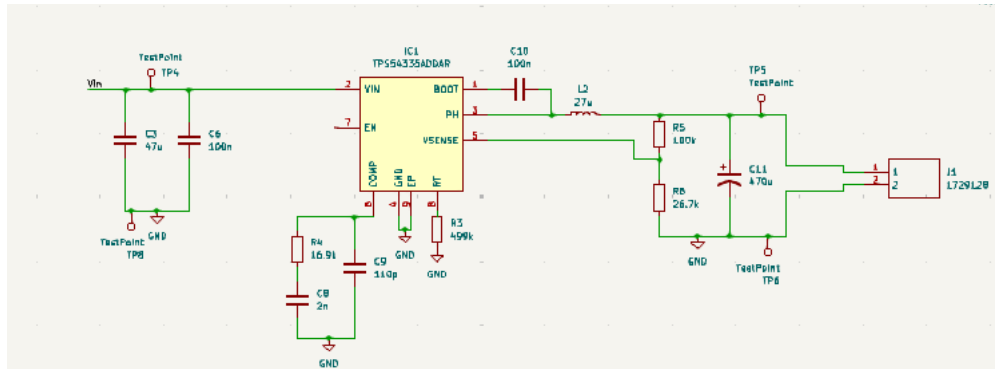


Figure 13: Synchronous Buck converter

2.2.5 Subsystem 5: Micro Controller Unit

This subsystem includes the ESP32 microcontroller responsible for sending a 100 kHz PWM signal to the gate driver (which controls MOSFET switches in Subsystem 1) and successful communication with both proximity sensors. It essentially allows for charging only when the drone is detected within our specified range by the proximity sensors. The entire subsystem is housed on our transmitting board and was coded using Arduino IDE.

The full schematic for the microcontroller unit can be seen in Figure 14 below.

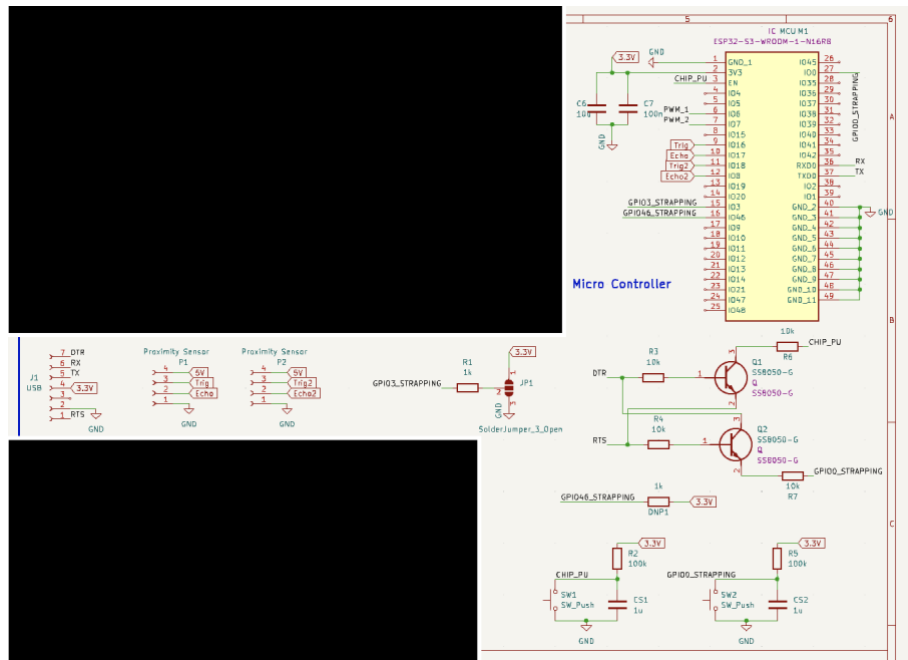


Figure 14: Microcontroller schematic

The external circuitry for the ESP-32 chip was needed for GPIO strapping that basically allowed the chip to download the code. This external circuitry consisted of buttons to allow for booting and resetting, a solder jumper, transistors, and a UART to USB connection. These are all mostly located on the right side of the figure, with the exception being the UART to USB connection being located on the left labeled “J1 USB.”

Both proximity sensors only had four pins which were as follows: voltage in, trigger, echo, and ground. The voltage input was 5 V from a linear regulator in Subsystem 1. Trigger and echo were used to send out and receive sound waves that would bounce off the target and allowed for calculations that would determine the distance away an object was. These two pins for each sensor were connected to I/O pins on the ESP-32 chip that allowed for these calculations.

3. Design Verification

We tested each of our subsystems independently with the help of equipment in the lab. We made use of oscilloscopes, signal/waveform generators, DC power supply, and other equipment. After having tested with the equipment, we then tested the systems together. However, one of our main subsystems didn't work and we were not able to get high voltages. So we just stuck with the individual system tests.

3.1 Two Step Inverter and Voltage Regulation

For this subsystem, one of the requirements as mentioned in Appendix A was to get the voltage regulators to work and output 3.3V, 5V and 12V. We were able to achieve this and we tested this with an oscilloscope.

We couldn't get the high side circuitry of the gate driver to work. This was one of the major failures of our project. The main reason for this was that the bootstrap capacitor was not high enough to boost the voltage of the signal. We were able to get the low side circuitry of the gate driver to work. This was a result we got for the low side circuitry. The drop in voltage in a cycle is due to the resistive load.

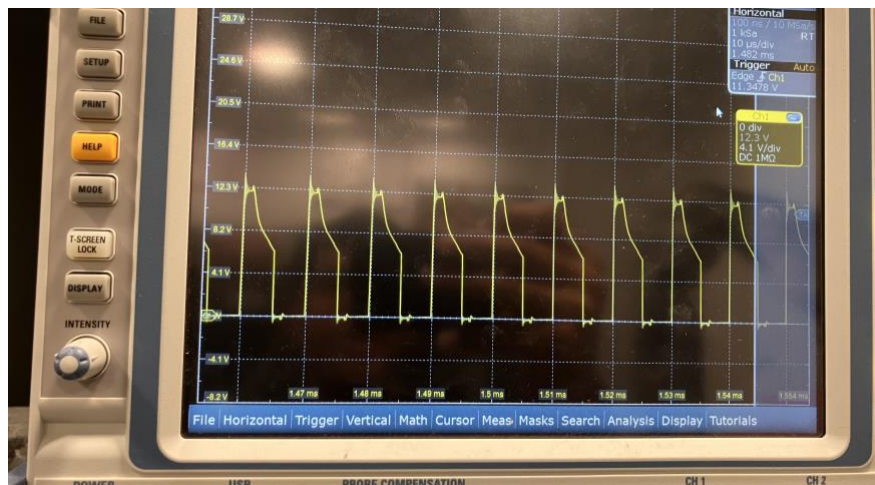


Figure 15: Square wave (low side gate driver circuitry)

Since the gate driver wasn't working we were not able to get the other two requirements to work as well.

3.2 Resonant Coils

We verified the bode plot of the coils with our setup. Figure 16 shows the Bode plot we got with our setup using a capacitance of $0.25\mu F$. The maximum value of the transfer function was at 120kHz

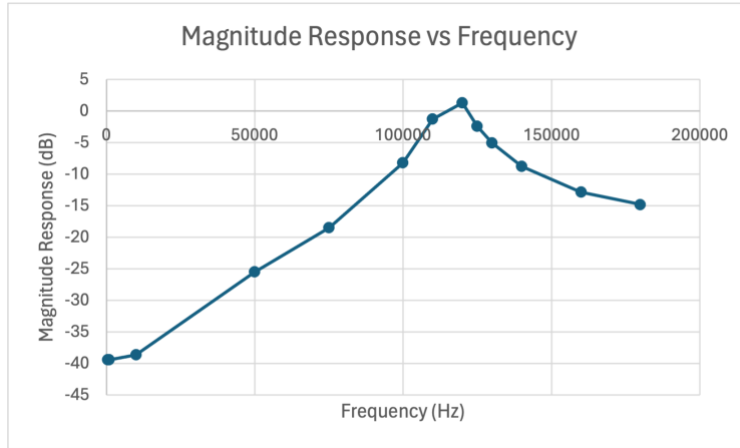


Figure 16: Bode plot for the LC resonant tank

Our system was working at 100kHz satisfying the 0.97dB as mentioned in the table in Appendix A. We were also able to get a sine wave on the receiving side(drone) of the same frequency. We couldn't test the power transfer since we were not able to get the high voltage input from the first subsystem.



Figure 17 and 18: Figure 17(left) shows the input which is a square wave. Figure 18(right) shows the output on the receiving side – a sine wave of the same frequency

3.3 Full Bridge Rectifier

The figures below show the verification of the full bridge rectifier. From these figures, we can see that a 10Vpp AC sine wave at 100kHz from the waveform generator resulted in a 5.222 V DC output. If we were able to receive the high AC voltage from the receiving coil, we would be able to get our prescribed 10 V DC output by modifying the smoothing capacitance and output resistance; thus, these subsystems proved to be a success. (Refer to Appendix A for the R&V table)

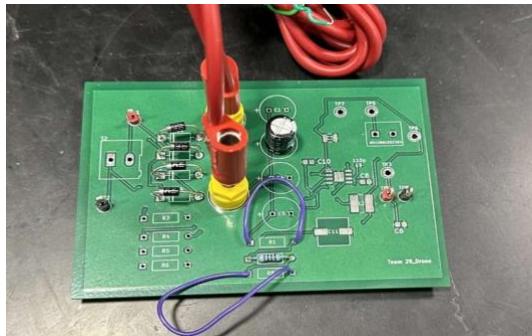


Figure 19: Full Bridge Rectifier PCB



Figure 20 and 21: Figure 20(left) shows input to the PCB we used. Figure 21(right) shows the output.

3.4 Synchronous Buck Converter with Voltage Regulation

The figures below show one test case for this subsystem. We can observe that a 15V DC input from the DC power supply resulted in a $3.8 \pm 3\%$ V DC. Input voltages ranging from 5V DC to 15 VDC were also tested, giving the same output. The output current was also measured using an oscilloscope and a resistive load, where its value was always less than 2A. As a result, all design requirements were met for this subsystem.

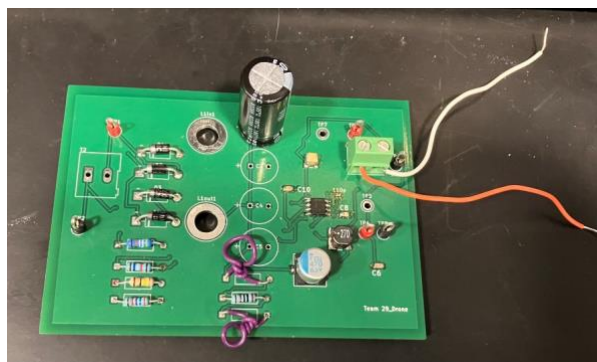


Figure 22: Synchronous Buck converter PCB



Figure 23 and 24: Figure 23(left) shows the input and Figure (24) shows the output we got.

3.5 Microcontroller Unit

The following figures show the verification of our requirements set for this subsystem that can be seen in Appendix A. First, Figure 25 shows the completed PCB for this subsystem. Figure 26 shows the serial monitor which displays that the ESP-32 chip and proximity sensors are properly communicating and that a PWM signal is active when within our set specific range. Figure 27 shows the PWM signals that are sent out by the ESP-32 that would have been used to drive the gate driver.



Figure 25: Microcontroller PCB

```

PWM Active
Distance1 (cm): 3.01
Distance2 (cm): 3.59
PWM Active
Distance1 (cm): 2.86
Distance2 (cm): 2.94
PWM Active
Distance1 (cm): 3.37
Distance2 (cm): 2.62
PWM Active
Distance1 (cm): 2.70
Distance2 (cm): 4.56
PWM Active
Distance1 (cm): 18.24
Distance2 (cm): 16.20
Distance1 (cm): 17.19
Distance2 (cm): 16.83
Distance1 (cm): 16.41
Distance2 (cm): 15.56
Distance1 (cm): 16.59
Distance2 (cm): 16.51
Distance1 (cm): 16.86
Distance2 (cm): 15.88
Distance1 (cm): 17.27

```

Figure 26: ESP-32 Serial Monitor with distances

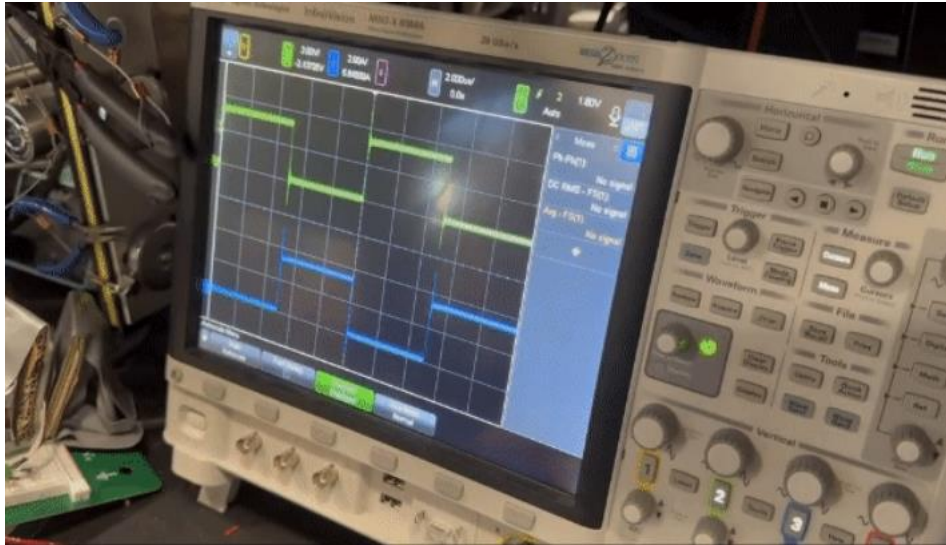


Figure 27: ESP-32 Output PWM Waveforms

4. Costs

The total cost of this project was calculated by adding the total of the parts table in Section 4.1 and the result of the labor cost found in Section 4.2. Our total comes out at \$36689.52. This does not include any shipping costs or the price of components or PCBs that were provided free of charge by the course.

4.1 Parts

Some parts were free or borrowed so they are not listed in the table below. The table lists any component that our budget or our own money was put towards.

Table 1: Parts Costs

Part (Quantity [Spare])	Manufacturer (Website)	Retail Cost (\$)	Quantity (Spare)	Actual Cost (\$)
Transmitting Coil	Wurth Electronics (DigiKey)	\$14.91	42 (41)*	\$14.91
Receiving Coil	Wurth Electronics (DigiKey)	\$14.83	1 (0)	\$14.83
1N4007 Diodes	Diodes Incorporated (DigiKey)	\$0.20	10 (6)	\$1.41
110 pF Capacitors	Murata Electronics (DigiKey)	\$0.17	3 (2)	\$0.51
47 uF Capacitors	Murata Electronics (DigiKey)	\$1.10	2 (1)	\$2.20
470 uF Capacitors	Chemi-Con (DigiKey)	\$0.87	4 (2)	\$3.48
Buck IC Chip	Texas Instruments (DigiKey)	\$1.91	2 (1)	\$3.82
1 kΩ Resistor	Yageo (DigiKey)	\$0.018	10 (9)	\$0.18
27 uH Inductor	Wurth Electronics (DigiKey)	\$1.88	2 (1)	\$3.76
26.7 kΩ Resistor	Vishay Dale (DigiKey)	\$0.026	10 (9)	\$0.26
16.9 kΩ Resistor	Vishay Dale (DigiKey)	\$0.026	10 (9)	\$0.26
100 kΩ Resistor	Vishay Dale (DigiKey)	\$0.026	10 (9)	\$0.26
499 kΩ Resistor	Vishay Dale (DigiKey)	\$0.026	10 (9)	\$0.26
0.1 uF Capacitor	Kemet (DigiKey)	\$0.056	10 (9)	\$0.56
2000 pF Capacitor	Kemet (Mouser)	\$0.48	2 (1)	\$0.96
IRLB4132PBF MOSFET	Infineon (Mouser)	\$0.761	10 (6)	\$7.61
LT1162 Gate Driver	Analog Devices Inc. (Mouser)	\$15.52	3 (2)	\$46.56

0.33 uF Capacitor	Kyocera AVX (Mouser)	\$0.275	10 (8)	\$2.75
3.3V Linear Regulator	Texas Instruments (Mouser)	\$0.59	5 (4)	\$2.95
12V Linear Regulator	STMicroelectronics (Mouser)	\$0.65	5 (4)	\$3.25
Proximity Sensor	SparkFun Electronics (Mouser)	\$3.95	1 (0)	\$3.95
10 kΩ Resistor	Yageo (DigiKey)	\$0.10	4 (3)	\$0.40
26.7 kΩ Resistor	Stackpole Electronics Inc. (DigiKey)	\$0.10	4 (3)	\$0.40
16.9 kΩ Resistor	Stackpole Electronics Inc. (DigiKey)	\$0.10	4 (3)	\$0.40
100 kΩ Resistor	Yageo (DigiKey)	\$0.10	4 (3)	\$0.40
499 kΩ Resistor	Yageo (DigiKey)	\$0.10	4 (3)	\$0.40
1000 uF Capacitor	Nichicon (DigiKey)	\$0.825	10 (6)	\$8.25
Terminal Block	Phoenix Contact (DigiKey)	\$0.77	4 (1)	\$3.08
3.7 V Lithium Battery	SparkFun Electronics (DigiKey)	\$5.50	2 (1)	\$11.00
4-pin Female L Connector	Sullins Connector Solutions (DigiKey)	\$0.56	4 (2)	\$2.24
Tactile Switch	CUI Devices (DigiKey)	\$0.18	4 (2)	\$0.72
USB to UART Board	Seeed Technology Co., Ltd (DigiKey)	\$7.95	1 (0)	\$7.95
Testpoints	Keystone Electronics (DigiKey)	\$0.308	25 (10)	\$7.70
BJT NPN Transistor	Comchip Technology (Mouser)	\$0.29	4 (2)	\$1.16
M3 Screws	Keystone Electronics (Mouser)	\$0.228	10 (2)	\$2.28
ESP32-S3-WROOM-1 Chip	Espressif Systems (DigiKey)	\$3.90	2 (1)	\$7.80
5 V Linear Regulator	STMicroelectronics (DigiKey)	\$0.74	4 (3)	\$2.96
7-pin Female L Connector	Sullins Connector Solutions (DigiKey)	\$0.72	2 (1)	\$1.44
1N4148 Diode	Onsemi (DigiKey)	\$0.057	10 (8)	\$0.57

24 SMD to DIP Socket Adapter	SchmalzTech LLC (DigiKey)	\$1.89	3 (2)	\$5.67
IRFZ44NPBF MOSFET	Infineon (Mouser)	\$0.889	10 (6)	\$8.89
110 pF Capacitor	Murata Electronics (Mouser)	\$0.108	10 (9)	\$1.08
Total				\$189.52

*Only one transmitting coil was ordered, but 42 were received

4.2 Labor

We estimate that each group member did about 120 hours of work over the semester. The total amount will come out to 120 hours * 3 group members = 360 hours to complete the project. Assuming an average UIUC graduate salary of \$40 per hour, the total labor cost can be calculated at $\$40 * 2.5 * 360 = \36000 .

The machine shop has given us the quote of 10 hours to complete the mechanical part of the project. If we assume a cost of \$50 per hour for machine shop work, the total machine shop cost can be calculated at $\$50 * 10 = \500 .

5. Conclusion

5.1 Accomplishments and Uncertainties

We were able to successfully demonstrate the wireless transfer of power. Our rectifier and buck converter circuits worked as expected and they were able to regulate the voltage to the desired values. The MCU was able to trigger the PWM waves based on the position of the drone and that was another big win for us. However, our gate driver could not drive the MOSFETs and so that was one main setback of our design.

5.2 Ethical considerations

Most ethical concerns to do with this project are more so about the drones and their enhanced capabilities when used with our wireless charger than the actual wireless charger itself. The biggest ethical concern to do with drones is privacy because they have the capability to record people without their knowledge or permission. Another ethical concern is the potential weaponization of drones. Drones are already used in combat, and cutting out the need for them to get plugged in in order to charge could make them more useful in this area. Our project is not intended to be used in either of these ways. It is, however, intended to be used for research purposes. This would create environmental ethical concerns such as noise and congestion issues. We would hope that the drones would be used in moderation to limit these concerns. The last potential ethical issue would be the loss of jobs as this technology would take over the need for people to charge the drone. We do not really foresee this becoming an issue.

There are a few safety issues to consider with both the drone and charger components of the project. The biggest potential issue would be the drone colliding with people or objects. This could be caused by control malfunction or, more related to our project, the battery runs out. There are also risks related to cybersecurity and drones getting hacked. The drone we will use will follow IEEE 1936.1-2021 for drone applications[1].

The charger safety issues include shock risks along with overheating leading to fire. The shock risk is our main concern in this project since we anticipate having exposed coils with live voltage running through them. We will make sure to follow appropriate standards to mitigate all risks involved with our project. This includes, but is not limited to, the "Interface definitions" (IEC PAS 63095-1: 2017) standard and the SAE J2954: 2020 which regulates wireless power charging[2].

The charger will be charging a 3.7 V lithium ion battery which also comes with some safety concerns. These include battery failure due to aging, thermal abuse, and electrical abuse[6]. Our group is aware of the possible risks and will abide by ISO 26262[7]. We have also signed off on the batteries training documentation provided by course staff. We are aware of the dangers of using a lithium battery and have selected a charging IC made for batteries to help mitigate some of the risk. We also are aware of the procedure if something goes wrong while testing the battery.

5.3 Future work

Going forward we would like to fix the issue with the gate driver and get the whole system to work. We have identified an alternate gate driver and if time permits we would like to try to get the gate driver working. With the gate driver working, we would be able to test our circuit with high voltages and get the whole system to work as intended. We would also like to integrate an automatic landing feature that would allow the drone to land on the charging pad whenever it comes in close vicinity (within 2-3m). This added feature would take us further close to our goal of charging the drone autonomously and would allow for more operation time without any human intervention.

References

- [1] "IEEE SA - IEEE standard for drone applications framework," IEEE Standards Association, <https://standards.ieee.org/ieee/1936.1/7455/> (accessed Feb. 7, 2024).
- [2] A. Marinescu, "Current Standards and Regulations for Wireless Battery Charging Systems," 2021 7th International Symposium on Electrical and Electronics Engineering (ISEEE), Galati, Romania, 2021, pp. 1-6, doi: 10.1109/ISEEE53383.2021.9628689. keywords: {Wireless communication;Roads;Inductive charging;Sociology;Regulation;Production facilities;Batteries;Wireless Power Charging;Standards and Regulation for Consumer Devices;EVs and PHEVs},
- [3] Resonant converter with coupling independent resonance for Wireless Power Transfer Application, <https://cpes.vt.edu/library/viewnugget/622#:~:text=Another%20challenge%20of%20the%20resonant,transfer%20standard%2C%20is%206.78MHz.> (accessed Feb. 8, 2024).
- [4] "Understanding LLC operation (part I): Power switches and resonant tank: Article: Mps," Article | MPS, <https://www.monolithicpower.com/understanding-llc-operation-part-i-power-switches-and-resonant-tank> (accessed Feb. 8, 2024).
- [5] A. Raciti, S. A. Rizzo, and G. Susinni, "Drone charging stations over the buildings based on a Wireless Power Transfer System," 2018 IEEE/IAS 54th Industrial and Commercial Power Systems Technical Conference (I&CPS), May 2018. doi:10.1109/icps.2018.8369967
- [6] X. Zhou, L. Cheng, Y. Wan, N. Qi, L. Tian and F. You, "Research on Lithium-ion Battery Safety Risk Assessment Based on Measured Information," 2020 IEEE Sustainable Power and Energy Conference (iSPEC), Chengdu, China, 2020, pp. 2047-2052, doi: 10.1109/iSPEC50848.2020.9351160. keywords: {Lithium-ion batteries;Temperature measurement;Voltage measurement;Thermal management;Battery charge measurement;Safety;Risk management;lithium-ion battery;thermal runaway;risk assessment;active safety}
- [7] S. S. Tikar, "Compliance of ISO 26262 safety standard for lithium ion battery and its battery management system in hybrid electric vehicle," 2017 IEEE Transportation Electrification Conference (ITEC-India), Pune, India, 2017, pp. 1-5, doi: 10.1109/ITEC-India.2017.8333870. keywords: {Batteries;ISO Standards;Hardware;Hazards;Software;Lithium;ISO 26262;Lithium ion battery;Battery

- management system;HARA;ASIL},
- [8] A. Agcal, S. Ozcira, and N. Bekiroglu, "Wireless Power Transfer by Using Magnetically Coupled Resonators," *www.intechopen.com*, Jun. 29, 2016. <https://www.intechopen.com/chapters/51254> (accessed Feb. 23, 2024).
- [9] Texas Instruments. (2018). TPS54335A 4.5V to 28V Input, 3A, 500kHz Step Down Converter [Datasheet]. Retrieved from <https://www.ti.com/lit/ds/symlink/tps54335a.pdf>
- [10] "15.6: Resonance in an AC Circuit," *Physics LibreTexts*, Nov. 01, 2016. [https://phys.libretexts.org/Bookshelves/University_Physics/University_Physics_\(OpenStax\)/Book%3A_University_Physics_II_-_Thermodynamics_Electricity_and_Magnetism_\(OpenStax\)/15%3A_Alternating-Current_Circuits/15.06%3A_Resonance_in_an_AC_Circuit](https://phys.libretexts.org/Bookshelves/University_Physics/University_Physics_(OpenStax)/Book%3A_University_Physics_II_-_Thermodynamics_Electricity_and_Magnetism_(OpenStax)/15%3A_Alternating-Current_Circuits/15.06%3A_Resonance_in_an_AC_Circuit)
- [11] On semiconductor is now - onsemi, <https://www.onsemi.com/pub/Collateral/AND9135-D.PDF> (accessed Feb. 23, 2024).
- [12] "H-bridge Control | Modular Circuits," Mar. 09, 2012. <https://www.modularcircuits.com/blog/articles/h-bridge-secrets/h-bridge-control/>
- [13] "Frequency Data as per AWG size in Litz Wire," *YDK Litz Wire & Cable*. <https://www.hflitzwire.com/frequency-as-per-awg-size/>
- [14] Electronics tutorials, "Series Resonance in a Series RLC Resonant Circuit," *Basic Electronics Tutorials*, Jun. 04, 2018. <https://www.electronics-tutorials.ws/accircuits/series-resonance.html>
- [15] Polycase, "DC-47P Heavy-Duty Electronics Enclosure," Polycase. https://www.polycase.com/dc-47p#DC-47PMBYT*01 (accessed May 29, 2024).
- [16] *LT1162ISW product Datasheet*. [Online]. Available: <https://www.mouser.com/datasheet/2/609/11602fb-3123592.pdf>. [Accessed: 28-Mar-2024]
- [17] "ESP32 with HC-SR04 ultrasonic sensor with Arduino Ide," Random Nerd Tutorials, <https://randomnerdtutorials.com/esp32-hc-sr04-ultrasonic-arduino/> (accessed Mar. 29,2024).

Appendix A Requirement and Verification Table

Table 2: System Requirements and Verifications

Subsystem	Requirement	Verification	Verification status (Y or N)
Subsystem 1: Two step inverter and Voltage Regulation	The output of the circuit is a square wave with voltages -24V and 24V	Input 24V DC and use an oscilloscope to check the waveform of the output	N
	The voltage supplied by the linear regulators match the specified value	Input 24V DC and check the output of the linear regulators with the help of an oscilloscope	Y
	All four MOSFETs in the full bridge inverter are driven at the correct switching frequency of 100 kHz .	This would be tested using the test points for select 1 and select 2 to make sure they are receiving the signal and that the signal is of a correct frequency. This is verifiable using an oscilloscope.	N
	Gate driver works properly and amplifies the input signals	This would be tested using an oscilloscope and checking the input and output waveforms.	N
Subsystem 2: Resonant Coils	The efficiency of the wireless power transmission should be more than 50%	Given an input AC, the input power on the transmission side and output power on the receiving side will be measured with the help of watt meters. The output power should be greater than 50% of the input power.	N
	The LC circuit on the transmission side should be operating within the 0.97 dB of the resonance frequency i.e. 125kHz.	We will check this by using a network analyzer. A network analyzer can determine the frequency response of the transmitting coil, ensuring it operates within the desired frequency range for efficient power transfer.	Y
	The distance between the coils should be less than 5cm	Checked physically with the help of a tape measure/ruler.	Y
Subsystem 3: Full Bridge Rectifier	The full bridge rectifier must be able to convert AC voltage from the WPF system to $10 \pm 3\%$ V DC.	We will use the variac, wattmeter, and oscilloscope in the lab to confirm this AC-DC conversion.	Y
Subsystem 4: Synchronous Buck Converter with Voltage Regulation	The TI buck converter should be able to convert $10 \pm 3\%$ V DC to regulated $3.8 \pm 3\%$ V DC.	This DC-DC conversion would be confirmed using a testbench DC power supply and oscilloscope.	Y
	The synchronous buck converter chip operates at 100 kHz switching frequency.	This would be confirmed using an oscilloscope.	Y
	Maximum output current of 2A.	This would be confirmed using current probes.	Y
	Successful dynamic regulation of output voltage.	We will use the testbench DC power supply to send low input voltages into the converter chip to verify that the chip can	Y

		control the duty ratio to maintain output voltage.	
Subsystem 5: Micro Controller Unit	Successful communication between proximity sensor and ESP32 microcontroller.	Confirmation that the proximity sensor distance data is being read through the use of serial printing onto the monitor.	Y
	Successful communication with the gate driver and the PWM signal has frequency of 100kHz.	Validated via serial printing onto the monitor.	Y
	Successful control of the transmitting circuit with I/O signal. Allow charging only when the drone is detected	Confirmed by observing the output of the MCU and the control circuit via an oscilloscope.	Y